Biosensors and Bioelectronics 72 (2015) 1–9

Contents lists available at ScienceDirect

Biosensors and Bioelectronics

journal homepage: www.elsevier.com/locate/bios

BODIPY-based azamacrocyclic ensemble for selective fluorescence detection and quantification of homocysteine in biological applications

Zan Li, Zhi-Rong Geng*, Cui Zhang, Xiao-Bo Wang, Zhi-Lin Wang*

State key Laboratory of Coordination Chemistry, School of Chemistry and Chemical Engineering, Collaborative Innovation Center of Advanced Microstructures, Nanjing University, Nanjing 210093, PR China

ARTICLE INFO

Article history:
Received 10 February 2015
Received in revised form
16 April 2015
Accepted 27 April 2015
Available online 28 April 2015

Keywords:
Fluorescent chemosensor
BODIPY
Azamacrocyclic Cu^{2+} ensemble
Homocysteine sensor
Hcy sensor
Cystathionine β-synthase activity

ABSTRACT

Considering the significant role of plasma homocysteine in physiological processes, two ensembles (F_{465}–Cu^{2+} and F_{508}–Cu^{2+}) were constructed based on a BODIPY (4,4-difluoro-1,3,5,7-tetramethyl-4-bora-3a,4a-diaza-s-indacene) scaffold conjugated with an azamacrocyclic (1,4,7-triazacyclononane and 1,4,7,10-tetraazacyclododecane) Cu^{2+} complex. The results of this effort demonstrated that the F_{465}–Cu^{2+} ensemble could be employed to detect homocysteine in the presence of other biologically relevant species, including cysteine and glutathione, under physiological conditions with high selectivity and sensitivity in the turn-on fluorescence mode, while the F_{508}–Cu^{2+} ensemble showed no fluorescence responses toward biothiols. A possible mechanism for this homocysteine-specific specificity involving the formation of a homocysteine-induced six-membered ring sandwich structure was proposed and confirmed for the first time by time-dependent fluorescence spectra, ESI-MS and EPR. The detection limit of homocysteine in deproteinized human serum was calculated to be 241.4 nM with a linear range of 0–90.0 μM and the detection limit of F_{465} for Cu^{2+} is 74.7 nM with a linear range of 0–6.0 μM (F_{508}, 80.2 nM, 0–7.0 μM). We have demonstrated the application of the F_{465}–Cu^{2+} ensemble for detecting homocysteine in human serum and monitoring the activity of cystathionine β-synthase *in vitro*.

© 2015 Elsevier B.V. All rights reserved.

1. Introduction

Biological thiols (biothiols) such as glutathione (GSH), cysteine (Cys) and homocysteine (Hcy) present in biological systems play vital roles in physiological processes, including protein structure and function maintenance, redox homeostasis control and detoxification (Ivanov et al., 2000; Wood et al., 2003). Altered levels of biothiols are associated with various physiological diseases (Murakami et al., 1989; Ross et al., 1997; Heafield et al., 1990; Refsum and Ueland, 1998).

Hcy is a key intermediate amino acid generated by the demethylation of methionine in S-adenosylmethionine-dependent transmethylation reactions (Langman and Cole, 1999). Hcy is metabolized mainly through a transsulfuration pathway catalyzed by cystathionine β-synthase (Stead et al., 2004). Plasma Hcy exists in three major forms, with trace amounts (~1%) existing in the reduced form. Approximately 70% is bound to albumin, and the remaining 30% forms low molecular weight disulfides predominantly with Cys. The sum of all these Hcy species is termed total Hcy (tHcy) (Ueland, 1995). Normal levels of fasting plasma tHcy in healthy adults are considered to be in the range of 5–15 μM (Ueland et al., 1993). However, impaired Hcy metabolism generally caused by cystathionine β-synthase deficiency results in excessive concentrations of tHcy (> 15 μM) in plasma and urine, a condition that is clinically diagnosed as hyperhomocysteinemia. Moderate, intermediate, and severe hyperhomocysteinemia refers to concentrations of 16–30, 31–100, and > 100 μM, respectively (Kang et al., 1992). The mechanism by which Hcy exerts its effect has not yet been clearly defined, but it is generally accepted that the elevated Hcy in plasma can damage the endothelium and induce vascular injury (Ozkan et al., 2002). Clinical and epidemiological studies have shown a relationship between elevated tHcy levels and coronary artery disease (Ozkan et al., 2002), stroke (Coull et al., 1990), and osteoporotic fractures (van Meurs et al., 2004). tHcy has also been linked to an increased risk of dementia and Alzheimer's disease (Seshadri et al., 2002), metabolic syndrome (Yakub et al., 2014), neural tube defects (Steegers-Theunissen et al., 1994) and pregnancy complications (Vollset et al., 2000). Consequently, assessment of tHcy levels in blood plasma and urine is of great clinical diagnostic significance.

Over the past decades, effective strategies have been developed for Hcy detection, and the methods are based mainly on chromatographic separation and enzyme immunoassay. The chromatographic

* Corresponding authors. Fax: +86 25 83317761
E-mail addresses: gengzr@nju.edu.cn (Z.-R. Geng), wangzl@nju.edu.cn (Z.-L. Wang).

http://dx.doi.org/10.1016/j.bios.2015.04.085
0956-5663/© 2015 Elsevier B.V. All rights reserved.

separation technique (Nekrassova et al., 2003; McMenamin et al., 2009) involves the derivatization of the sulfhydryl group, requiring tedious separation techniques such as gas chromatography with mass spectrometry (GC/-MS) and high performance liquid chromatography (HPLC), thus limiting the ability of Hcy to function as an important biomarker. Enzyme immunoassay (Shipchandler and Moore, 1995; Pernet et al., 2000; Newton et al., 2010) requires the use of the commercially available kits, using enzymes, antibodies and biomolecules that are expensive and intrinsically labile, generally using multi-step addition and washing procedures with specialized storage conditions. The instruments are typically sophisticated to operate. Therefore, there is an urgent need to develop simple and inexpensive methods for Hcy detection.

Fluorescence probing serves as the most attractive approach to monitor biologically relevant species because of its sensitivity and simplicity. In recent years, numerous fluorescent probes have been developed to distinguish biothiols from other amino acids (Guy et al., 2007; Yi et al., 2009; Lim et al., 2011; Lee et al., 2012; Zhang et al., 2011; Shao et al., 2012). However, due to the high degree of similarity of both structures and the reactivity among the biothiols, the reports on the selective detection of Hcy over Cys/GSH were addressed relatively seldom (Barve et al., 2014; Lee et al., 2014; Peng et al., 2014).

The Cu^{2+}-based ensemble is comprised of a Cu^{2+} center and a specific fluorescent molecule. Because of the strong quenching ability of paramagnetic Cu^{2+} for fluorophores, the ensemble is generally non-fluorescent after incorporating Cu^{2+} (Liu et al., 2013). As far as we know, the Chang group first reported the ensemble composed of fluorescein-dipicolylamine and Cu^{2+} for selective fluorescence responds of the sulfide anion (Choi et al., 2009). To date, the Cu^{2+}-based ensembles have been developed rapidly for sensing varied analytes such as sulfide (Sasakura et al., 2011; Fu et al., 2014), cyanide (Guliyev et al., 2009; Lou et al., 2012), and histidine (You et al., 2014; Reddy et al., 2014). However, these chemosensors all relied on the high affinity between Cu^{2+} and the analyte, and biothiols easily interfered with the detection of the analyte. Considering the critical role of biothiols in maintaining the redox status of biological systems, there are to date few cases of ensembles for probing biothiols utilizing a redox reaction. To our best knowledge, the Yang group reported a spiropyran-based ensemble for Hcy/Cys (Shao et al., 2006). No other Cu^{2+}-based ensemble is reported for the selective sensing of biothiols, especially Hcy. Therefore, to exploit a novel Hcy chemosensor based on a Cu^{2+} ensemble has become a current research challenge.

We designed and synthesized two ensembles (F_{465}–Cu^{2+} and F_{508}-Cu^{2+}) based on a BODIPY scaffold conjugated with an azamacrocyclic Cu^{2+} complex, employing 1,4,7-triazacyclononane (TACN) and 1,4,7,10-tetraazacyclododecane (Cyclen), (Schemes 1a, b). F_{465}–Cu^{2+} can be employed to detect Hcy in the presence of Cys/GSH under physiological conditions with high sensitivity and selectivity in the turn-on fluorescence mode. We have then demonstrated an application of F_{465}–Cu^{2+} for Hcy detection in a real human plasma sample, which offers a potential application in the clinical diagnosis of coronary disease. We have also utilized the F_{465}–Cu^{2+} ensemble to monitor cystathionine β-synthase activity *in vitro*, thus establishing a methodology to evaluate cystathionine β-synthase activity and delivering a potential tool to regulate Hcy

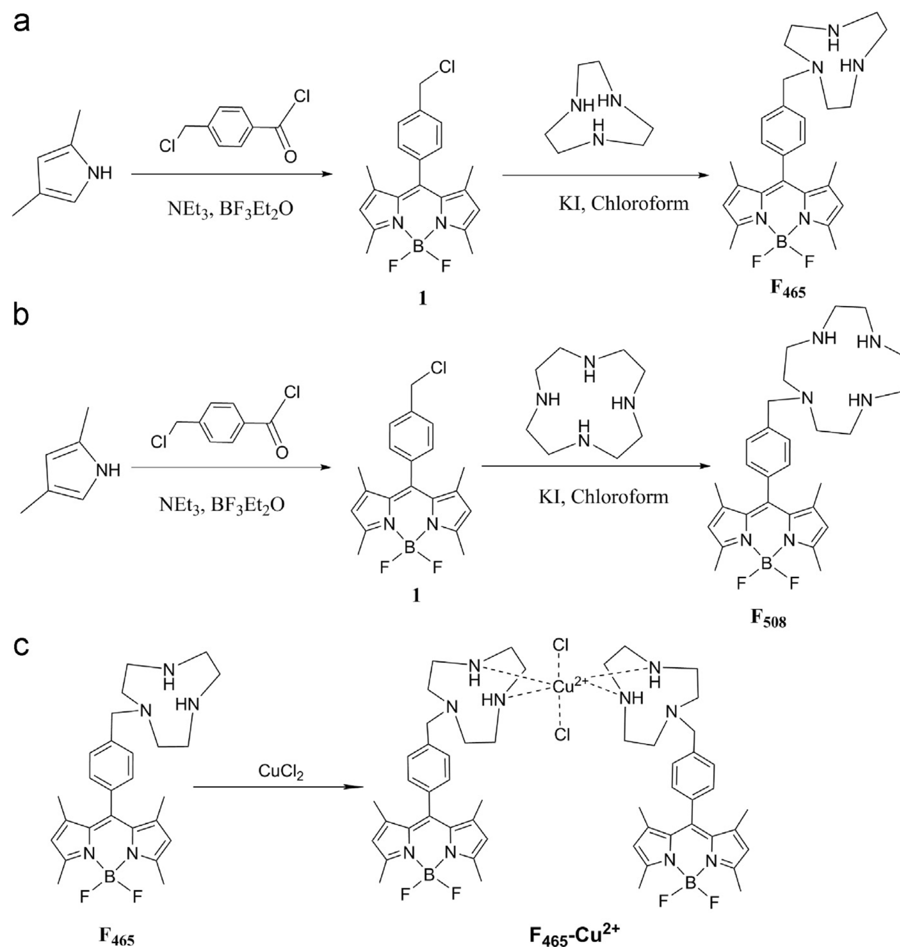

Scheme 1. Synthetic procedure for F_{465}, F_{508} and F_{465}–Cu^{2+}.

levels in biological fluids.

2. Materials and methods

2.1. Reagents and materials

L-Homocysteine (≥ 98%), L-serine (≥ 99%), pyridoxal 5′-phosphate hydrate (≥ 98%), glutathione (≥ 98%), cysteine (≥ 98%), D L-homocysteine (≥ 95%), KO_2, sodium nitroprusside dihydrate (≥ 99%), 2,2′-azobis(2-amidinopropane) dihydrochloride (AAPH, 97%) and $BF_3 \cdot OEt_2$ (46%) were obtained from Sigma-Aldrich (St. Louis, MO, USA), 2,4-Dimethyl-1H-pyrrole (≥ 98%), tert-butyl hydroperoxide (TBHP, 70%) and 4-(chloromethyl)benzoyl chloride (≥ 98%) were purchased from Adamas-Beta (Basle, MO, Switzerland). Copper chloride dihydrate ($CuCl_2 \cdot 2H_2O$, 98%), hydrogen peroxide solution (30%), sodium hypochlorite solution (8%), amino acids, petroleum ether (AR), ethyl acetate (AR), chloroform (AR), methanol (AR) and ethanol (AR) were purchased from Sinopharm (Shanghai, China) and used without further purification. 1,4,7-triazacyclononane and 1,4,7,10-tetraazacyclododecane were obtained from Dibo Chem (Shanghai, China); ct-DNA and BSA (98%) were purchased from KeyGen (Nanjing, China). Dichloromethane (AR) and triethylamine (AR) were distilled before use.

2.2. Apparatus

NMR spectra were measured on a Bruker DRX-500 spectrometer at 25 ± 1 °C with TMS as the internal standard and chloroform as the solvent. EPR spectra were determined using a Bruker EMX-10/12 spectrometer. Electro-spray ionization mass spectra were measured on an LCQ Fleet Thermo Fisher mass spectrometer. Fluorescence spectra were determined on a PerkinElmer LS55 fluorescence spectrometer. Absorption spectra were determined on a UV-3600 Shimadzu UV–vis-NIR spectrometer. A Lauda E100 circulating water pump was used to maintain a constant temperature at 37 °C. Ultrapure water was prepared using a Milli-Q A10 system.

2.3. Synthesis

2.3.1. 8-(Chlorobenzyl)-4,4-difluoro-1,3,5,7-tetramethyl-4-bora-3a,4a-diaza-s-indacene

(compound 1)

2,4-Dimethyl-1H-pyrrole (2.756 g, 29.01 mmol) and 4-(chloromethyl)benzoyl chloride (2.75 g, 14.55 mmol) were dissolved in 300 ml of dichloromethane under N_2. The resulting solution was stirred at room temperature under N_2 for 2 h. Triethylamine (4.24 g, 42.0 mmol) was added and the mixture was stirred for 15 min. Then, $BF_3 \cdot OEt_2$ (2.64 ml) was added. The solution was then stirred for 2 h at room temperature. The green organic solution was washed with brine and dried over anhydrous Na_2SO_4. The crude product was purified on a silica gel column, eluting with petroleum ether and ethyl acetate (4:1) to yeild a brick red powder 2.60 g (50%) (Li et al., 2013).

2.3.2. 8-[4-(1,4,7-Triazacyclononane-1-yl)benzyl]-4,4-difluoro-1,3,5,7-tetramethyl-4-bora-3 a,4 a-diaza-s-indacene (F_{465})

Compound 1 (380 mg, 1.02 mmol) and 1,4,7-triazacyclononane (1.29 g, 10.0 mmol) were added to 60 ml chloroform. The resulting mixture was stirred for 24 h under N_2 at room temperature. After the solution was concentrated, the residue was re-dissolved in dichloromethane and washed three times with brine. The organic phase was dried over anhydrous Na_2SO_4. The residue was purified by silica gel column chromatography (chloroform: methanol (20: 1)) to afford a red solid (436.61 mg, 92%). ^1H NMR (500 MHz, $CDCl_3$) δ 7.48 (*d*, *J*=8.0, 2H), 7.25 (*d*, *J*=7.9, 2H), 5.99 (s, 2H), 3.82 (s, 2H), 3.00 (s, 2H), 2.86 (s, 4H), 2.74 (s, 4H), 2.73 – 2.69 (m, 4H), 2.56 (s, 6H), 1.40 (s, 6H). ^{13}C NMR (126 MHz, $CDCl_3$) δ 155.40, 143.01, 141.61, 140.41, 133.88, 131.46, 129.83, 128.04, 121.20, 61.42, 52.63, 46.26, 46.09, 14.56, 14.41. ESI -MS (CH_3OH): Calcd. for F_{465} [$F_{465}+H^+$] 466.40, found 466.75.

2.3.3. 8-[4-(1,4,7,10-Tetraazacyclododecane-1-yl)benzyl]-4,4-difluoro-1,3,5,7-tetramethyl-4-bora-3 a,4 a-diaza-s-indacene (F_{508})

Compound 1 (330 mg, 0.887 mmol) and 1,4,7,10-tetraazacyclododecane (1.51 mg, 8.78 mmol) were added to 70 ml chloroform. The resulting mixture was stirred for 5 h under N_2 at room temperature. After the solution was concentrated, the residue was re-dissolved in dichloromethane and washed three times with brine. The organic phase was dried over anhydrous Na_2SO_4. The residue was purified by silica gel column chromatography (chloroform: methanol (10: 1)) to afford a red solid (400.75 mg, 89%).^1H NMR (500 MHz, $CDCl_3$) δ 7.46 (*d*, *J*=8.0, 2H), 7.26 (*d*, *J*=8.1, 2H), 5.99 (s, 2H), 3.79 (s, 2H), 2.89 – 2.84 (m, 4H), 2.75 (*d*, *J*=5.0, 4H), 2.70 (s, 4H), 2.68 – 2.62 (m, 4H), 2.57 (s, 6H), 1.88 (s, 3H), 1.41 (s, 6H). ^{13}C NMR (126 MHz, $CDCl_3$) δ 155.34, 143.14, 141.73, 139.69, 133.64, 129.64, 128.00, 121.16, 58.99, 51.46, 47.41, 46.33, 45.39, 29.69, 14.53. ESI-MS (CH_3OH): Calcd. for F_{508} [$F_{508}+H^+$] 509.47, found 509.75.

2.3.4. Preparation of F–Cu^{2+} ensembles

F_{465} (4.65 mg, 1.0 mmol) was dissolved in 5 ml of ethanol, and 1 ml of $CuCl_2 \cdot 2H_2O$ (136.4 mg, 0.8 mmol) ethanol solution was dropped slowly into solution accompanied with the formation of a dark red precipitate. Then, the mixture was stirred at room temperature for 12 h. The dark red precipitate was filtered and washed three times with ethanol and dried under vacuum. ESI-MS (CH_3OH): Calcd. for F_{465}–Cu^{2+} [$2F_{465}+CuCl_2+H^+$] 1066.24, found 1066.42 (Fig. S7a).

2.4. Preparation of the stock solution

The stock solution of F_{465}–Cu^{2+} and F_{508}–Cu^{2+} was prepared at 200 μM and diluted with Tris–HCl buffer (20 mM, pH 7.4) to 10 μM. The stock solutions of other substrates were all prepared in deionized water before fluorescence spectral analyses were performed. The generation of ROS/RNS was performed as described (see Supporting information). All the fluorescence spectra were measured in Tris–HCl buffer (20 mM, pH 7.4).

2.5. Pretreatment of the human blood sample

Human sera were separated from the blood of healthy people, and serum from coronary disease patients was acquired from Nanjing Jiangbei Renmin Hospital (Nanjing, China). Written informed consent was obtained from individual subjects. Protein in the serum was precipitated by the addition of ethanol and followed by centrifugation (12,000 rpm) for 20 min (Sreejith et al., 2008). The reduced Hcy (trace amounts) contained in the supernatant liquid was collected and oxidized by appropriate GSSG to exclude the interference of Hcy in the serum for obtaining a baseline. Collected serum (2 ml) was vigorously mixed with the appropriate amount of $NaBH_4$ and incubated for 20 min at room temperature to reduce the protein-bound and free oxidized Hcy (Reddy et al., 2014). The protein in the reduced sample was then precipitated by the addition of ethanol, followed by centrifugation (12,000 rpm) for 20 min. The supernatant liquid containing Hcy was collected and used for quantification studies.

2.6. The activity assay of cystathionine β-synthase (CBS)

The recombinant cystathionine β-synthase (CBS; EC 4.2.1.22; >95% purity) was expressed in *Escherichia coli*. To optimize the reaction conditions, the reaction mixture (100 μl), containing pyridoxal 5′-phosphate (45 μM), L-serine (6 mM), L-homocysteine (1.5 mM), CBS (0, 0.05, 0.15, 0.25, 0.35, 0.45, 0.55, 0.65, 0.75, 0.85, 0.95, 1.05, 1.15, 1.25 mg/ml) in Tris–HCl (100 mM, pH 8.6) was incubated in a capped tube at 37 °C for 10 min, and then 100 μl of ethanol was added to quench the reaction in an ice bath. The resultant solution was added into the solution of F_{465}–Cu^{2+} (10 μM, pH 7.4) and incubated for 30 min before the fluorescence was measured.

To determine the activity of cystathionine β-synthase (CBS), the standard reaction was performed in the presence of 100 μl of reaction solution containing pyridoxal 5′-phosphate (45 μM), L-serine (6 mM), L-homocysteine (0, 0.75, 1.50, 2.25, 3.0, 3.75, 4.50, 5.25, 6.0 mM) and CBS (0.05 mg/ml) in Tris–HCl (100 mM, pH 8.6). At the same time, the control experiment was performed using deactivated CBS (heated in boiling water for 10 min) under the same conditions for comparison.

3. Results and discussion

3.1. Design and synthesis of F_{508}, F_{465} and the preparation of F–Cu^{2+}ensembles

Boron-dipyrromethenes (BODIPYs) are very popular fluorophores with stable absorption, fluorescence emission and large extinction coefficients (Loudet and Burgess, 2007). Azamacrocyclic rings form stable metal complexes with Cu^{2+} (Fabbrizzi et al., 1996). Considering the characteristics of boron-dipyrromethenes (BODIPYs) (Loudet and Burgess, 2007) and azamacrocyclic rings, we combined BODIPY (4, 4-difluoro-1,3,5,7-tetramethyl-4-bora-3a,4a-diaza-s-indacene) and the metal chelators 1,4,7-triazacyclononane and 1,4,7,10-tetrazacyclododecane and formed a new type of fluorescent chemosensor for copper ions (Schemes 1a, b). We utilized the strong quenching ability of copper ions (Fabbrizzi et al., 1996) and the high quantum yields of F_{465} (Φ 0.316) and F_{508} (Φ 0.299) to form weak fluorescent F_{465}–Cu^{2+} (Φ 0.041) (Scheme 1c) and F_{508}–Cu^{2+} (Φ 0.033) ensembles. The ensembles were envisaged to be reduced by biothiols such as Cys, Hcy and GSH, which could switch on the fluorescence by disrupting the photo-induced electron-transfer (PET) process (de Silva et al., 1997).

3.2. Fluorescence response of F_{465} and F_{508} toward Cu^{2+}

To demonstrate the potential of F_{465} and F_{508} to be assembled with Cu^{2+} as a turn-on fluorescent probe, we evaluated the binding properties of F_{465} and F_{508} toward Cu^{2+} in Tris–HCl buffer (20 mM, pH 7.4). The emission spectra of F_{465} and F_{508} are not influenced in the pH range of 6.0-9.0 (Fig. S12), indicated their stability in the physiological environment. A strong emission peak at 512 nm was observed with the quantum yield (Φ) 0.316 in Tris–HCl buffer (20 mM, pH 7.4) (Fig. S1). The fluorescence intensity at 512 nm decreased gradually upon titrating with increasing concentrations of Cu^{2+} with F_{465} (Fig. S1). Moreover, the Job's plot indicated a 1: 2 binding stoichiometry between Cu^{2+} and F_{465} (F_{508}) (Fig. S2). The 1: 2 binding mode of Cu^{2+} and F_{465} (Scheme 1c) was further confirmed by the ESI-MS (Fig. S7a). The species of $[2F_{465}+CuCl_2+H^+]$ with m/z 1066.42 indicated the existence of the F_{465}-Cu^{2+} ensemble and m/z 1134.75 indicated the existence of $[2F_{508}+CuCl^+ +H_2O]$ (Fig. S7b).

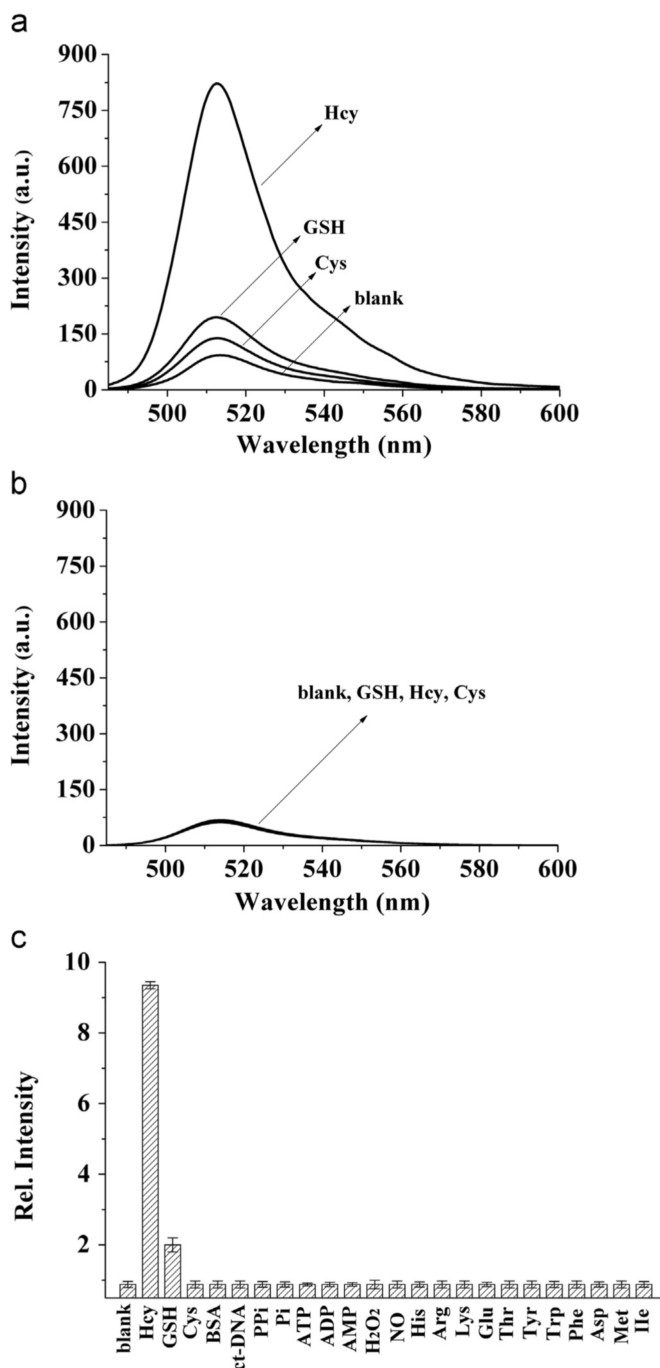

Fig. 1. (a) Fluorescence responses of 10 μM of the F_{465}–Cu^{2+} ensemble in the absence and presence of 20 equivalents of GSH, Cys, Hcy; (b) Fluorescence responses of 10 μM of the F_{508}–Cu^{2+} ensemble in the absence and presence of 20 equivalents of GSH, Cys, Hcy; (c) Fluorescence responses of F_{465}–Cu^{2+} (10 μM) to the biologically relevant substrates in Tris–HCl buffer (20 mM, pH 7.4). Biothiols (20 equivalents); Amino acids (100 equivalents); others analytes (100 equivalents). The data represents the average of three independent experiments. The error bars represent ± S.D. Fluorescence spectra were recorded 30 min after the addition of varied analyte. All measurements were taken at 37 °C in Tris–HCl buffer (20 mM, pH 7.4), slit width 2.5 nm. Excitation wavelength was 470 nm.

3.3. Fluorescence response of the two ensembles (F_{508}-Cu^{2+} and F_{465}-Cu^{2+}) toward biothiols

Both F_{508} and F_{465} are BODIPY-based azamacrocyclic fluorescent molecules. The apparent binding constant (K_s) of F_{465}–Cu^{2+} is $3.41\times10^4\ M^{-1}$ (the K_s of F_{508}–Cu^{2+} is $3.92\times10^4\ M^{-1}$) based on the Benesi–Hildebrand plots (Fig. S15, S16) (Fu et al., 2014). The

chelating ability for Cu^{2+} differes in spite of their similar structures. Because the biothiols were envisaged to reduce the copper of the ensembles to form cuprous complexes, the recovery of the fluorescence quenched by Cu^{2+} thus furnished a turn-on sensor (Rigo et al., 2004; Sasakura et al., 2011). Based on our strategy, we tested the fluorescence response of F_{508}–Cu^{2+} and F_{465}–Cu^{2+} toward Cys, Hcy and GSH. As shown in Fig. 1b, at the excitation wavelength of 470 nm in Tris–HCl buffer (20 mM, pH 7.4), 10 μM F_{508}–Cu^{2+} exhibited no fluorescence changes with addition of 20 equiv. Hcy, Cys and GSH after 30 min while 10 μM F_{465}–Cu^{2+} showed dramatic fluorescence enhancement after adding 20 equivalents of Hcy. In contrast, no significant changes in emission intensity were caused by addition of 20 equivalents of Cys and GSH (Fig. 1a). The different binding constant of F_{508}–Cu^{2+} (K_s $3.92\times10^4\ M^{-1}$) and F_{465}–Cu^{2+} (K_s $3.41\times10^4\ M^{-1}$) may contribute to the exceptional fluorescence responses toward various biothiols under the same conditions. The kinetic study of F_{465}–Cu^{2+} (10 μM) toward Hcy (10 equivalents) was conducted under pseudo-first-order conditions (Yang et al., 2014), and the calculated observed rate constant (K_{obs}) was determined to be $0.155\pm\ 0.003\ min^{-1}$ (Fig. S17, S18), showing that F_{465}–Cu^{2+} is highly susceptible to the sulfhydryl group of the Hcy. In comparative research on the reducing ability of GSH, Cys and Hcy with dehydroascorbic acid (DHA), Hcy could function as a relatively potent reducing agent to promote significant reduction of DHA compared to Cys and GSH at a smaller order of magnitude in concentration (Park, 2001). This reaction also explained the selective response toward Hcy in our study. The effects of pH on F_{465}–Cu^{2+} were also investigated. As illustrated in Fig. S13, this probe displays a corresponding fluorescence enhancement in the pH range of 2.5–5.0, whereas the probe is quite stable up to pH 5.0, which clearly demonstrates the stability of our probe in the physiological pH range.

3.4. Selectivity and competition studies for tHE f_{465}-Cu^{2+} ensemble

To further test the specificity of our probe towards Hcy, fluorescence spectra of F_{465}–Cu^{2+} were recorded before and after addition of various amino acids, such as His, Glu, Arg, Lys, Glu, Thr, Tyr, Trp, Phe, Asp, Met, and IIe as well as biothiols (Hcy, Cys and GSH) (Fig. 1c), and various reactive oxygen/nitrogen species (ROS/RNS) (Fig. S5). In addition, the selectivity toward biologically relevant substrates ATP, ADP, AMP and PPi, Pi, the DNA, protein simulant ct-DNA and BSA was also studied. As shown in Fig. 1c, only Hcy causes an observable fluorescent response under identical conditions. Importantly, the other amino acids and species do not promote observable changes even when present in excess of 100 equivalents. These results suggest that the probe F_{465}–Cu^{2+} is highly selective for Hcy.

In addition, the competitive selectivity of the F_{465}–Cu^{2+} ensemble toward Hcy in the presence of other biologically relevant substrates was also evaluated by measuring the fluorescence changes at 512 nm upon addition of an excess amount of substrates under physiological conditions. The F_{465}–Cu^{2+} ensemble could respond to Hcy even in the presence of other substrates (Fig. S6). Therefore, this Hcy-selective sensor was not affected by relevant biological molecules indicating the excellent selectivity of the F_{465}–Cu^{2+} ensemble toward Hcy over other competitive substrates. Furthermore, fluorescence titration experiments were performed in Tris–HCl buffer solution (20 mM, pH 7.4), as shown in Fig. 2a. F_{465}-Cu^{2+} could react with increasing equiv. of Hcy (0-9 equivalents.), and a concentration-dependent fluorescence enhancement at 512 nm was recorded after 30 min. Based on these data, a calibration curve was obtained (Fig. 2b), with a linear range of 0–90 μM supporting the potential use of this probe for detecting Hcy at low concentrations.

3.5. Proposed mechanism for sensing Hcy

Previous work has demonstrated that copper ions could be reduced by biothiols under physiological conditions. This process results in the formation of cuprous complexes and disulfide (Rigo et al., 2004; Shao et al., 2006). We anticipate that the fluorescence response of F_{465}–Cu^{2+} toward Hcy could be a consequence of a redox reaction in which Cu^{2+} in the ensemble is reduced to the Cu^{+} species by Hcy. Because Hcy has one extra methylene group compared to Cys, according to the reported pKa values of sulfhydryl groups in biothiols, Hcy is 8.87 and Cys is 8.0 (Reddy et al., 2014). In this case, Cys is deprotonated more easily than Hcy in basic buffer solutions. As shown in Scheme 2a, the deprotonated Hcy in physiological solutions could react with F_{465}–Cu^{2+} thus generating a six-membered sandwich structure while Cys forms a five-membered ring (Scheme 2b). The intramolecular cyclization to form a six-membered ring with Hcy should be kinetically favored relative to the formation of the five-membered ring that Cys formed (Chen et al., 2013; Hakuna et al., 2014). As a result, the six-membered ring is more stable than the five-membered ring in this study. Previous reports revealed that dissolved molecular oxygen could oxidize the Cu^{+} complex to a Cu^{2+} complex with generation of superoxide ions (Scarpa et al., 1996). The six-membered sandwich structure is kinetically more stable than the five-membered structure with the oxidation of dissolved molecular oxygen, therefore creating a distinct fluorescence response. To gain experimental support for this proposal, time-dependent fluorescence changes of F_{465}–Cu^{2+} toward Hcy were studied, as shown in Fig. 2c, upon addition of 20 equivalents of GSH, Cys and Hcy to the solution of 10 μM F_{465}–Cu^{2+} in Tris–HCl buffer (20 mM, pH 7.4). The fluorescence response differed dramatically. Hcy elicited increasing fluorescence intensity in the course of time, which reached a maximum (approximately 10-fold) at 30 min, indicating that F_{465}-Cu^{2+} was reduced by Hcy to form the kinetically favored six-membered structure. Compared to Hcy, Cys also induced the fluorescence enhancement and reached a maximum at 18 min, then decreasing fluorescence followed, eventually reaching a minimum at 30 min. This phenomenon supported our hypothesis that F_{465}–Cu^{2+} was reduced to form the five-membered sandwich structure that was not favored kinetically and was quickly oxidized by dissolved molecular oxygen, probably catalyzed by trace Cu^{2+} in the solution (Rigo et al., 2004), with fluorescence quenching due to formation of the Cu^{2+} complex. GSH promoted a slight (approximately 2-fold) fluorescence response. The pKa of GSH is 9.20, which is higher than Hcy and Cys (Reddy et al., 2014) and is also consistent with a minute fluorescence response toward GSH in this study. These fluorescence data fit well with our assumption. To shed light on the proposed six-membered ring assumption, the ESI-MS spectra were monitored after the reaction between Hcy and F_{465}-Cu^{2+}. The signal at m/z 1127.25 represents the $[2F_{465}+Cu^{+}+Hcy]$ species (Fig. S8) and demonstrates the existence of six-membered sandwich structure described in Scheme 2a.

Finally, reactions of F_{465}–Cu^{2+} with Hcy and Cys were explored, and the EPR spectra of F_{465}–Cu^{2+} in the absence and presence of Hcy and Cys were recorded (Fig. S14). Solution spectra of F_{465}-Cu^{2+} were isotropic with a g of 2.0631, while in the presence of Cys, g is 2.0637. Interestingly, the EPR spectrum of F_{465}–Cu^{2+} in the presence of Hcy with g is 2.0491, significantly different from Cys. As reported, Cu^{2+} could be reduced to Cu^{+} by Hcy and Cys (Rigo et al., 2004; Shao et al., 2006). The significant distinction in the EPR spectra between Hcy- and Cys- treated F_{465}–Cu^{2+} was ascribed to the difference between the Cu^{+} and the Cu^{2+} species. The previously mentioned six-membered ring formed by Hcy is kinetically stable in the form of Cu^{+} species, while the five-membered ring formed by Cys that is not kinetically favored could

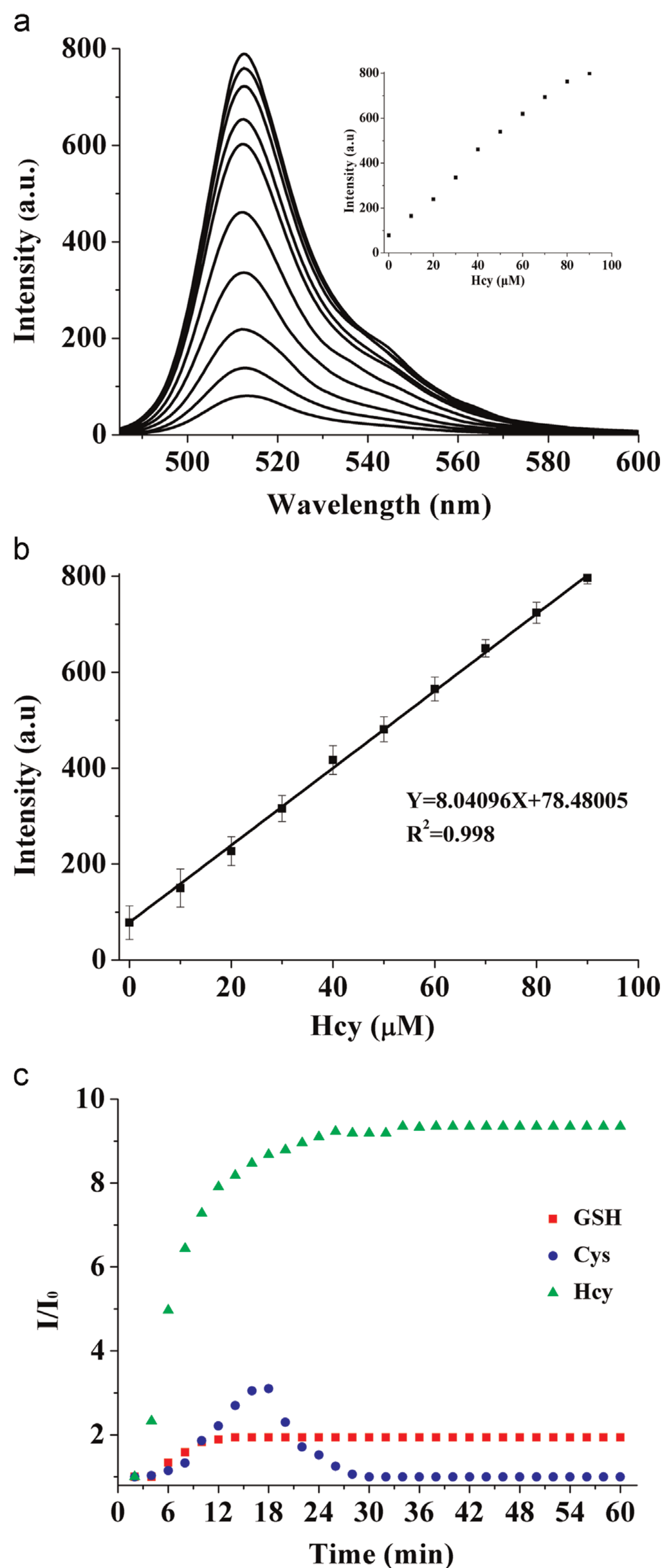

Fig. 2. (a) Concentration-dependent fluorescence changes of the F_{465}–Cu^{2+} ensemble (10 μM) toward spiked Hcy (0–90 μM) in Tris–HCl buffer solution (20 mM, pH 7.4). Inset: Changes of the fluorescence intensity at 512 nm upon the titration of Hcy; (b) Linear calibration curve of 10 μM F_{465}–Cu^{2+} as a function of the spiked Hcy (0–90 μM) in Tris–HCl buffer (20 mM, pH 7.4). The data represent the average of three independent experiments. The error bars represent ± S.D.; (c) Time-dependent relative fluorescence intensity of F_{465}-Cu^{2+} (10 μM) in Tris–HCl buffer (20 mM, pH 7.4) with addition of 20 equivalents of GSH, Cys and Hcy. All measurements were taken at 37 °C, slit width 2.5 nm. Excitation wavelength was 470 nm.

be oxidized by the dissolved molecular oxygen and thus exists as the Cu^{2+} species (Scheme 2). All of the results described above supported the proposed reaction with Hcy and further confirmed the distinct fluorescence response pathways toward Hcy and Cys.

3.6. Applications for detecting Hcy in the serum of coronary disease patients

Inspired by the above experimental results and considering the significance of Hcy in biological fluids, we studied the application of F_{465}–Cu^{2+} to human blood serum (HBS). In diluted deproteinized healthy HBS (10%), the concentration-dependent fluorescence enhancement of F_{465}–Cu^{2+} was observed with the addition of Hcy. A good linear calibration curve (R^2=0.996) was obtained, suggesting the potential utility of F_{465}-Cu^{2+} in HBS. A detection limit was calculated based on $3\sigma/s$, where σ is the standard deviation of blank measurements, and s is the slope of the linear regression curve. The detection limit of Hcy in deproteinized HBS was calculated to be 241.4 nM (Fig. 3a).

The elevated plasma Hcy levels are a risk factor for coronary heart disease (Ozkan et al., 2002). Currently, the Hcy has been used to clinically diagnose coronary heart diseases (Refsum et al., 2004). Subsequently, we utilized the probe for Hcy detection in the serum of a healthy person and a coronary disease patient. Because the GSH concentration in plasma is as low as 2 μM (Jones et al., 1998), the interference from GSH could be ignored (Fig. 1a). The Cys levels in the human plasma of healthy individuals range from 135.8 to 266.5 μM (Jacobsen et al., 1994) and are typically 20 times higher than normal Hcy levels, so the influence of Cys could also be ignored based on our fluorescence data above (Fig. 1a). Our study incorporated the standard addition method. This method consists of spiking varying standard amounts of Hcy into each diluted serum sample. The serum sample had previously been divided into several aliquots of equal volume. The results were represented as a plot with the concentration on the x axis and the fluorescence intensity on the y axis (Fig. 3b). Based on our method, the concentrations of Hcy in the serum of coronary disease patients were determined to be 36.02 ± 3.02 μM, RSD 8.38%. This value is in agreement with results measured using the commercially available Human Hcy ELISA kit (the measured value is 34.00 ± 0.77 μM, RSD 2.26%. Fig. S19). Both of the results measured are under the concentration range of 31–100 μM, defined as intermediate hyperhomocysteinemia (Kang et al., 1992), which proved that the Hcy levels in the serum of coronary disease patient was elevated. The assessment of serum Hcy for healthy people was also achieved utilizing the fluorescence assay and the ELISA kit (Fig. S20), also indicating the capacity of the F_{465}–Cu^{2+} ensemble in serum Hcy detection. These results demonstrated that our method allows the application of Hcy quantification in the serum of coronary disease patients with high selectivity and sensitivity.

3.7. Evaluating the activities of cystathionine β-synthase (Cbs)

Cystathionine β-synthase (CBS) is a pivotal enzyme that regulates Hcy homeostasis through the transsulfuration pathway, catalyzing the conversion of homocysteine and serine to cystathionine and deactivating the mutations in the CBS gene that are the primary cause of clinical CBS deficiency, a metabolic disorder characterized as extremely elevated tHcy in plasma (Gupta et al., 2008). Despite the vital role of CBS activity in human health, relatively few methods are available to evaluate its activity. As far as we know, the traditional methodology is radioisotope assay, which requires liquid chromatography/-mass spectrometry (LC/-MS) techniques (Kraus et al., 1978). We have developed a novel method using a fluorescence chemosensor to evaluate CBS activity.

This method is based on the principle that cystathionine β-

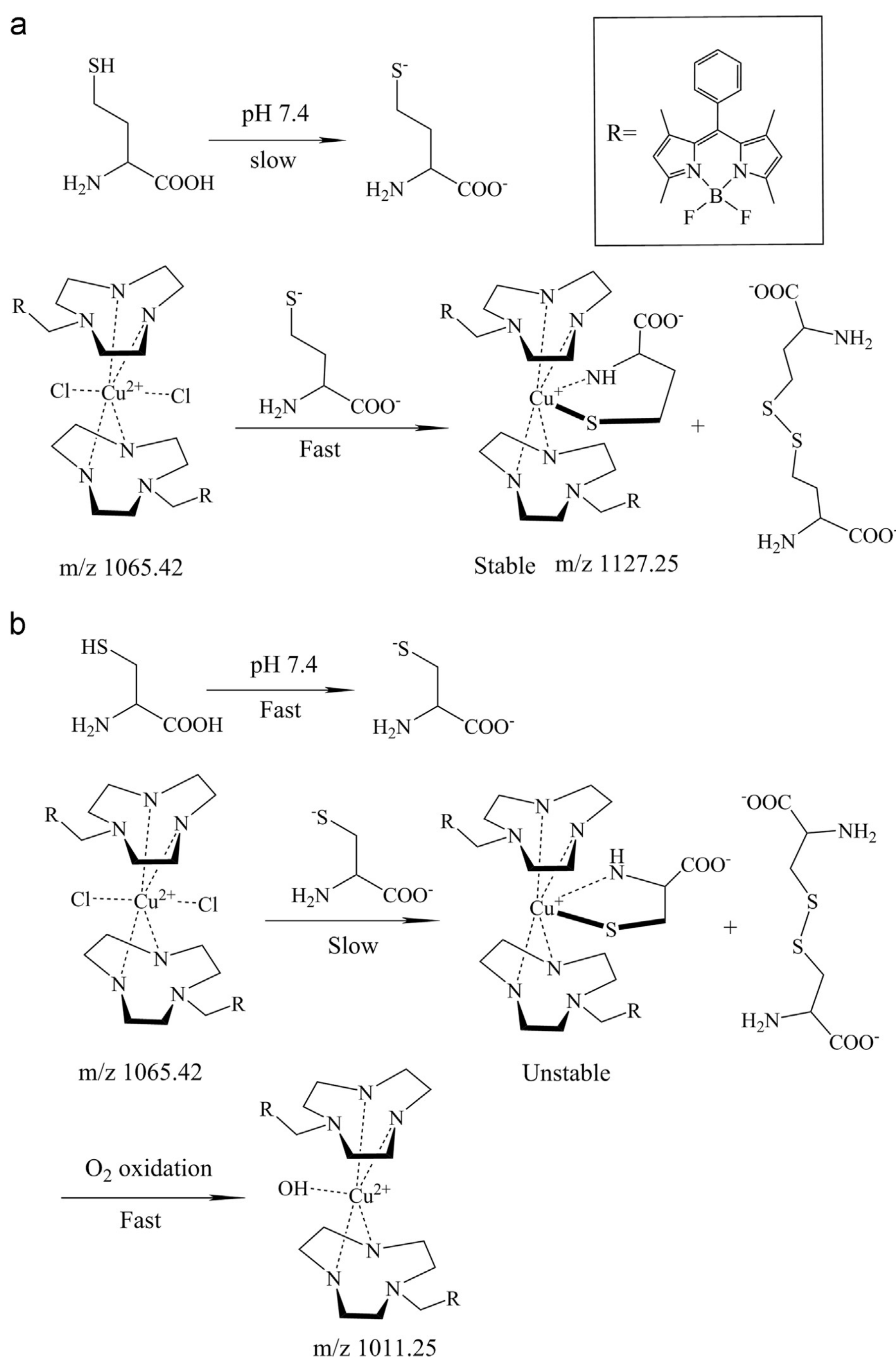

Scheme 2. Proposed sensing mechanism of F_{465}–Cu^{2+} for Hcy (a) and Cys (b).

synthase (CBS) could catalyze the conversion of homocysteine and serine to cystathionine with cofactor of PLP (Scheme S1), thus consuming Hcy under appropriate conditions. F_{465}–Cu^{2+} could detect Hcy when the Hcy was not used up by the CBS, so the CBS activity evaluation could be achieved by the quantification of Hcy utilizing the F_{465}–Cu^{2+} ensemble.

To optimize the reaction conditions, the fluorescence intensity of F_{465}–Cu^{2+} at various CBS concentrations was investigated. As shown in Fig. 4a, significant fluorescence enhancement was observed when adding the solution containing L-serine, L-homocysteine and pyridoxal 5′-phosphate (PLP). No fluorescence response was observed after the incubation of solutions containing CBS (0.05 mg/ml), L-serine, L-homocysteine and pyridoxal 5′-phosphate (PLP), indicating that Hcy was completely consumed by the CBS to form cystathionine. With the increasing concentrations of CBS (0.05–1.25 mg/ml), the fluorescence intensity was gradually elevated, which means catalyzing activity was relatively low when CBS was present in high concentrations, demonstrating that the optimum concentration of CBS was 0.05 mg/ml. When the control experiments were performed using deactivated CBS under the same conditions, the fluorescence enhancement was consistent with the blank group when deactivated CBS was added (Fig. S21). This outcome further confirmed the availability of the F_{465}–Cu^{2+} ensemble.

To determine the activity of cystathionine β-synthase (CBS), we then studied the time-dependent catalyzing activity of CBS. As shown in Fig. 4b, there was negligible fluorescence response of F_{465}–Cu^{2+} when the enzymatic reaction time was 10 min,

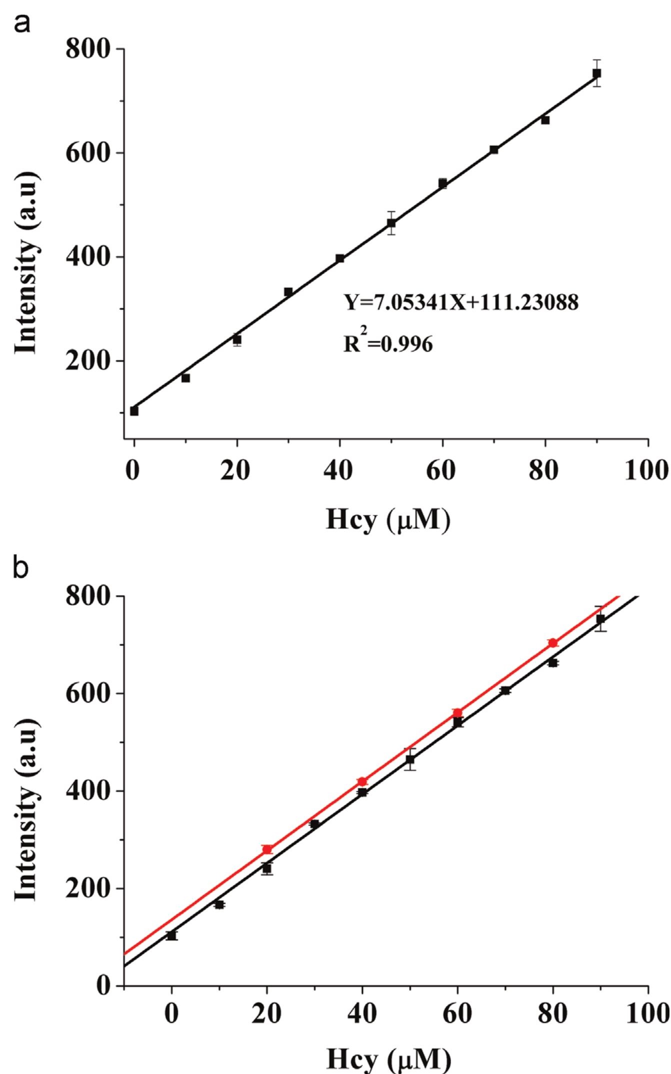

Fig. 3. (a) Linear calibration curve of 10 μM F_{465}–Cu^{2+} as a function of spiked Hcy from 0 to 90 μM in diluted deproteinized healthy HBS (containing 10% HBS). Fluorescence intensities at 512 nm were recorded 30 min after spiking Hcy; (b) Linear calibration curve of 10 μM F_{465}–Cu^{2+} as a function of spiked Hcy at 20 μM, 40 μM, 60 μM, 80 μM in diluted deproteinized serum of coronary disease patients (10% HBS) (upper line); Linear calibration curve of intensity versus spiked Hcy in diluted deproteinized healthy HBS (10% HBS) (bottom line). Fluorescence intensities at 512 nm were recorded 30 min after spiking Hcy and serum. The data represents the average of three independent experiments. The error bars represent ± S.D.

indicating that CBS could catalyze 6 mM L-homocysteine and equimolar L-serine to form cystathionine in the presence of pyridoxal 5′-phosphate (PLP). When the enzymatic reaction time was 5 min, 3.75 mM L-homocysteine was transformed to cystathionine by CBS. Only 2.25 mM L-homocysteine was consumed when the reaction time was 2 min. One unit of enzyme activity (U) is defined as the amount of CBS that catalyzes the formation of 1 μmol of cystathionine in 1 h at 37 °C (Kery et al., 1999), and the calculated activity of CBS according to the fluorescence data in this study was 6.75 ± 0.08 μU, RSD 1.19%. Significantly, our method needs less than 1 h and is relatively facile compared with the traditional radioisotope assay that utilizes LC/-MS techniques. These results indicate the excellent capacity of F_{465}–Cu^{2+} for monitoring cystathionine β-synthase (CBS) activity *in vitro*.

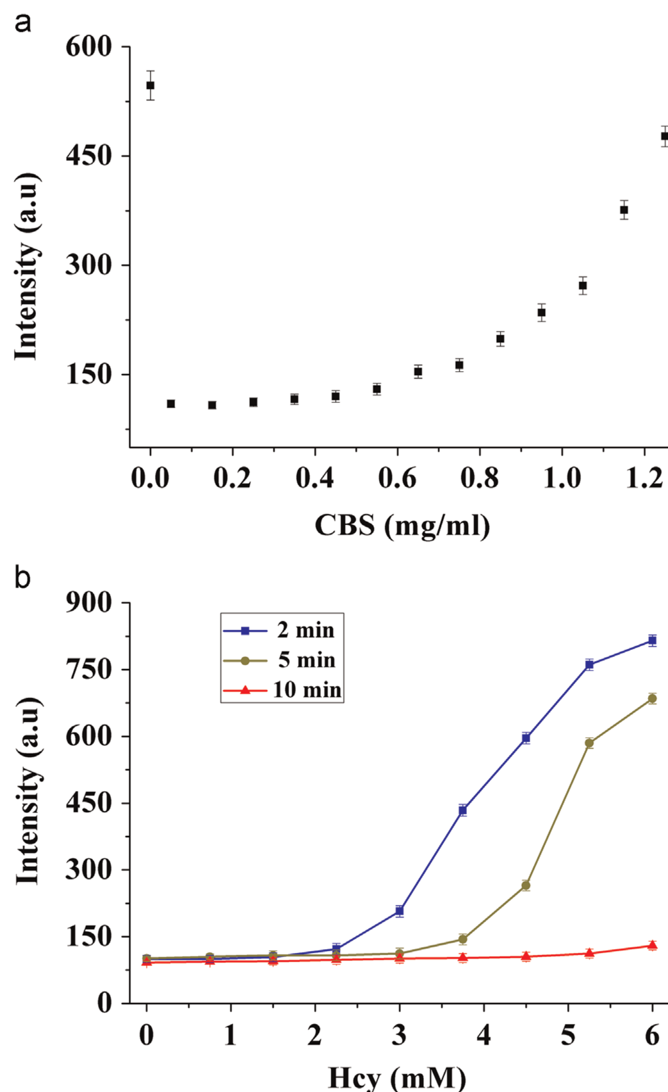

Fig. 4. (a) Fluorescence intensity of F_{465}–Cu^{2+} (10 μM) as a function of varied CBS concentrations (0, 0.05, 0.15, 0.25, 0.35, 0.45, 0.55, 0.65, 0.75, 0.85, 0.95, 1.05, 1.15, 1.25 mg/ml). The reaction solution consisted of L-serine (6 mM), L-homocysteine (1.5 mM) and pyridoxal 5′-phosphate (45 μM); (b) Fluorescence intensity of F_{465}–Cu^{2+} (10 μM) as a function of various concentrations of Hcy (0, 0.75, 1.50, 2.25, 3.0, 3.75, 4.50, 5.25, 6.0 mM). The reaction solutions consisted of CBS (0.05 mg/ml), L-serine (6 mM) and pyridoxal 5′-phosphate (45 μM). A different solid line represents varied enzymatic reaction times: 2 min, 5 min, 10 min. Fluorescence intensities at 512 nm were recorded 30 min after adding the solution. The data represents the average of three independent experiments. The error bars represent ± S.D.

4. Conclusions

In summary, we have designed and synthesized two ensembles (F_{465}–Cu^{2+} and F_{508}–Cu^{2+}) based on a BODIPY scaffold conjugated with an azamacrocyclic Cu^{2+} complex. The ensembles were envisaged to have the Cu^{2+} center reduced to Cu^{+} in the BODIPY-based azamacrocyclic ring when biothiols were encountered, thus switching on the fluorescence emissions by disrupting the photo-induced electron-transfer process. The results demonstrated that the F_{465}–Cu^{2+} ensemble could be employed to detect homocysteine in the presence of other biologically relevant species, including cysteine and glutathione in a turn-on fluorescence mode, while the F_{508}–Cu^{2+} ensemble exhibited no fluorescence response toward biothiols, attributed to the different binding constant between F_{465}–Cu^{2+} and F_{508}–Cu^{2+}. The homocysteine-specific detection mechanism of the F_{465}–Cu^{2+} ensemble

was demonstrated by the formation of a homocysteine-induced six-membered ring sandwich structure that resisted the oxidation of the molecular oxygen compared with the cysteine-induced five-membered ring structure. We have also demonstrated the application of the F_{465}–Cu^{2+} ensemble for detecting homocysteine in human serum and developed a useful methodology to evaluate the activities of cystathionine β-synthase *in vitro*.

Acknowledgements

This work is supported by the National Basic Research Program of China (2013CB922102), the National Natural Science Foundation of China (21275072, 21201101 and 21475059) and the Natural Science Foundation of Jiangsu Province (BK20130560).

Appendix A. Supplementary material

Supplementary data associated with this article can be found in the online version at http://dx.doi.org/10.1016/j.bios.2015.04.085.

References

Barve, A., Lowry, M., Escobedo, J.O., Huynh, K.T., Hakuna, L., Strongin, R.M., 2014. Chem. Commun. 50, 8219–8222.
Chen, H.L., Li, X.K., Bai, R.C., Wu, Y.B., Fan, Y.F., Chao, J.B., 2013. Organometallics 32, 6226–6231.
Choi, M.J., Cha, S.Y., Lee, H., Jeon, H.L., Chang, S.K., 2009. Chem. Commun., 7390–7392.
Coull, B.M., Malinow, M.R., Beamer, N., Sexton, G., Nordt, F., Garmo, Pd, 1990. Stroke 21, 572–576.
de Silva, A.P., Gunaratne, H.Q.N., Gunnlaugsson, T., Huxley, A.J.M., McCoy, C.P., Rademacher, J.T., Rice, T.E., 1997. Chem. Rev. 97, 1515–1566.
Fabbrizzi, L., Licchelli, M., Pallavicini, P., Perotti, A., Taglietti, A., Sacchi, D., 1996. Chem. Eur. J 2, 75–82.
Fu, Y., Feng, Q.C., Jiang, X.J., Xu, H., Lia, M., Zang, X.Q., 2014. Dalton Trans. 43, 5815–5822.
Guliyev, R., Buyukcakir, O., Sozmen, F., Bozdemir, O., 2009. Tetrahedron Lett. 50, 5139–5141.
Gupta, S., Wang, L.Q., Hua, X., Krijt, J., Kozich, V., Kruger, W.D., 2008. Hum. Mutat. 29, 1048–1054.
Guy, J., Caron, K., Dufresne, S., Michnick, S.W., Skene, W.G., Keillor, J.W., 2007. J. Am. Chem. Soc. 129, 11969–11977.
Hakuna, L., Escobedo, J.O., Lowry, M., Barve, A., McCallum, N., Strongin, R.M., 2014. Chem. Commun. 50, 3071–3073.
Heafield, M.T., Fearn, S., Steventon, G.B., Waring, R.H., Williams, A.C., Sturman, S.G., 1990. Neurosci. Lett. 110, 216–220.
Ivanov, A.R., Nazimov, I.V., Baratova, L., 2000. J. Chromatogr. A 895, 157–166.
Jacobsen, D.W., Gatautis, V.J., Green, R., Robinson, K., Savon, S.R., Secic, M., Ji, J., Otto, J.M., Taylor, L.M., 1994. Clin. Chem. 40, 873–881.
Jones, D., Carlson, J., Samiec, P., Sternberg, P., Mody, V., Reed, R., Brown, L., 1998. Clin. Chim. Acta 275, 175–184.
Kang, S.S., Wong, P.W.K., Malinow, M.R., 1992. Annu. Rev. Nutr. 12, 279–298.
Kery, V., Poneleit, L., Meyer, J.D., Manning, M.C., Kraus, J.P., 1999. Biochemistry 38, 2716–2724.
Kraus, J.P., Packman, S., Fowler, B., Rosenberg, L.E., 1978. J. Biol. Chem. 253, 6523–6528.
Langman, L.J., Cole, D.E.C., 1999. Crit. Rev. Clin. Lab. Sci. 36, 365–406.
Lee, H.Y., Choi, Y.P., Kim, S., Yoon, T., Guo, Z., Lee, S., Swamy, K.M.K., Kim, G., Lee, J.Y., Shin, I., Yoon, J., 2014. Chem. Commun. 50, 6967–6969.
Lee, M.H., Han, J.H., Kwon, P.S., Bhuniya, S., Kim, J.Y., Sessler, J.L., Kang, C., Kim, J.S., 2012. J. Am. Chem. Soc. 134, 1316–1322.
Lim, C.S., Masanta, G., Kim, H.J., Han, J.H., Kim, H.M., Cho, B.R., 2011. J. Am. Chem. Soc. 133, 11132–11135.
Liu, Z.P., He, W.J., Guo, Z.J., 2013. Chem. Soc. Rev. 42, 1568–1600.
Li, Z., Chen, Q.Y., Wang, P.D., Wu, Y., 2013. RSC Adv 3, 5524–5528.
Loudet, A., Burgess, K., 2007. Chem. Rev. 107, 4891–4932.
Lou, X.D., Ou, D.X., Lia, Q.Q., Li, Z., 2012. Chem. Commun. 48, 8462–8477.
McMenamin, M.E., Himmelfarb, J., Nolin, T.D., 2009. J. Chromatogr. B: Anal. Technol. Biomed. Life Sci. 877, 3274–3281.
Murakami, K., Kondo, T., Ohtsuka, Y., Fujiwara, Y., Shimada, M., Kawakami, Y., 1989. Metabolism 38, 753–758.
Nekrassova, O., Lawrence, N.S., Compton, R.G., 2003. Talanta 60, 1085–1095.
Newton, L.A.A., Sandhu, K., Livingstone, C., Leslie, R., Davis, J., 2010. Expert Rev. Mol. Diagn. 10, 489–500.
Ozkan, Y., Ozkan, E., Simsek, B., 2002. Int. J. Cardiol. 82, 269–277.
Park, J.B., 2001. Biochim. Biophys. Acta 1525, 173–179.
Peng, H.J., Wang, K., Dai, C.F., Williamson, S., Wang, B.H., 2014. Chem. Commun. 50, 13668–13671.
Pernet, P., Lasnier, E., Vaubourdolle, M., 2000. Clin. Chem. 46, 1440–1441.
Reddy, G., Agarwalla, U., Taye, H., Ghorai, N., Chattopadhyay, S., Das, A., S., 2014. Chem. Commun. 50, 9899–9902.
Refsum, H., Smith, A.D., Ueland, P.M., Nexo, E., Clarke, R., McPartlin, J., Johnston, C., Engbaek, F., Schneede, J., McPartlin, C., Scott, J.M., 2004. Clin. Chem. 50, 3–32.
Refsum, H., Ueland, P.M., 1998. Annu. Rev. Med. 49, 31–62.
Rigo, A., Corazza, A., di Paolo, M.L., Rossetto, M., Ugolini, R., Scarpa, M., 2004. J. Inorg. Biochem. 98, 1495–1501.
Ross, E.A., Koo, L.C., Moberly, J.B., 1997. Am. J. Kidney Dis. 30, 489–494.
Sasakura, K., Hanaoka, K., Shibuya, N., Mikami, Y., Kimura, K., Komatsu, T., Ueno, T., Terai, T., Kimura, H., Nagano, T., 2011. J. Am. Chem. Soc. 133, 18003–18005.
Seshadri, S., Beiser, A., Selhub, J., Jacques, P.F., Rosenberg, I.H., D'Agostino, R.B., Wilson, P.W.F., Wolf, P.A., 2002. N. Engl. J. Med. 346, 476–483.
Sreejith, S., Divya, K.P., Ajayaghosh, A., 2008. Angew. Chem. Int. Ed. 47, 7883–7887.
Scarpa, M., Momo, F., Viglino, P., Vianello, F., Rigo, A., 1996. Biophys. Chem. 60, 53–61.
Shao, J., Sun, H., Guo, H., Ji, S., Zhao, J., Wu, W., Yuan, X., Zhang, C., James, T.D., 2012. Chem. Sci. 3, 1049–1061.
Shao, N., Jin, J.Y., Cheung, M.S., Yang, R.H., Chan, W.H., Mo, T., 2006. Angew. Chem. Int. Ed. 118, 5066–5070.
Shipchandler, M.,T., Moore, E.,G., 1995. Clin. Chem. 41, 991–994.
Stead, L.M., Jacobs, R.L., Brosnan, M.E., Brosnan, J.T., 2004. Adv. Enzyme Regul. 44, 321–333.
Steegers-Theunissen, R.P.M., Boers, G.H.J., Trijbels, F.J.M., Finkelsteina, J.D., Bloma, H. J., Thomasa, C.M.G., Borma, G.F., Woutersa, M.G.A.J., Eskesa, T.K.A.B., 1994. Metabolism 43, 1475–1480.
Ueland, P.M., Refsum, H., Stabler, S.P., Malinow, M.R., Andersson, A., Allen, R.H., 1993. Clin. Chem. 39, 1764–1779.
Ueland, P.M., 1995. Clin. Chem. 41, 340–342.
van Meurs, J.B.J., Dhonukshe-Rutten, R.A.M., Pluijm, S.M.F., van der Klift, M., M.D., de Jonge, R., Lindemans, J., de Groot, L.C.P.G.M., Hofman, A., Witteman, J.C.M., van Leeuwen, J.P.T.M., Breteler, M.M.B., Lips, P., Pols, H.A.P., Uitterlinden, A.G., 2004. N. Engl. J. Med. 350, 2033–2041.
Vollset, S.E., Refsum, H., Irgens, L.M., Emblem, B.M., Tverdal, A., Gjessing, H.K., Bjorke Monsen, A.L., Ueland, P.M., 2000. Am. J. Clin. Nutr. 71, 962–968.
Wood, Z.A., Schroder, E., Harris, J.R., Poole, L.B., 2003. Trends Biochem. Sci. 28, 32–40.
Yakub, M., Schulze, K.J., Khatry, S.K., Stewart, C.P., Christian, P., West, K.P., 2014. Nutrients 6, 1649–1661.
Yang, X.F., Huang, Q., Zhong, Y.G., Li, Z., Li, H., Lowry, M., Escobedo, J.O., Strongin, R. M., 2014. Chem. Sci. 5, 2177–2183.
Yi, L., Li, H., Sun, L., Liu, L., Zhang, C., Xi, Z., 2009. Angew. Chem. Int. Ed. 48, 4034–4037.
You, Q.H., Lee, W.A., Chan, W.H., Zhu, X.M., Leung, K.C., 2014. Chem. Commun. 50, 6207–6210.
Zhang, J., Shibata, A., Ito, M., Shuto, S., Ito, Y., Mannervik, B., Abe, H., Morgenstern, R., 2011. J. Am. Chem. Soc. 133, 14109–14119.